

Shape modulation of squaramide-based supramolecular polymer nanoparticles

Citation for published version (APA):

Saez Talens, V., Makurat, D. M. M., Liu, T., Dai, W., Guibert, C., Noteborn, W. E. M., Voets, I. K., & Kieltyka, R. E. (2019). Shape modulation of squaramide-based supramolecular polymer nanoparticles. *Polymer Chemistry*, 10(23), 3146-3153. <https://doi.org/10.1039/c9py00310j>

Document license:
TAVERNE

DOI:
[10.1039/c9py00310j](https://doi.org/10.1039/c9py00310j)

Document status and date:
Published: 21/06/2019

Document Version:
Publisher's PDF, also known as Version of Record (includes final page, issue and volume numbers)

Please check the document version of this publication:

- A submitted manuscript is the version of the article upon submission and before peer-review. There can be important differences between the submitted version and the official published version of record. People interested in the research are advised to contact the author for the final version of the publication, or visit the DOI to the publisher's website.
- The final author version and the galley proof are versions of the publication after peer review.
- The final published version features the final layout of the paper including the volume, issue and page numbers.

[Link to publication](#)

General rights

Copyright and moral rights for the publications made accessible in the public portal are retained by the authors and/or other copyright owners and it is a condition of accessing publications that users recognise and abide by the legal requirements associated with these rights.

- Users may download and print one copy of any publication from the public portal for the purpose of private study or research.
- You may not further distribute the material or use it for any profit-making activity or commercial gain
- You may freely distribute the URL identifying the publication in the public portal.

If the publication is distributed under the terms of Article 25fa of the Dutch Copyright Act, indicated by the "Taverne" license above, please follow below link for the End User Agreement:

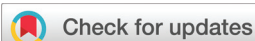
www.tue.nl/taverne

Take down policy

If you believe that this document breaches copyright please contact us at:

openaccess@tue.nl

providing details and we will investigate your claim.



Cite this: *Polym. Chem.*, 2019, **10**, 3146

Shape modulation of squaramide-based supramolecular polymer nanoparticles†

Victorio Saez Talens,^a D. M. M. Makurat,^a Tingxian Liu,^a Wei Dai,^a Clément Guibert,^b Willem E. M. Noteborn,^a Ilja K. Voets ^b and Roxanne E. Kieltyka ^{*a}

We report the synthesis and self-assembly of a library of squaramide-based bolaamphiphiles with variable hydrophobic and hydrophilic domain sizes, consisting of varied aliphatic chains ($n = 2$ to 12 methylene repeat units) and linear oligo(ethylene glycol) ($m = 11$ to 36 repeat units), to understand their effect on the formation of supramolecular polymer nanoparticles. Systematic variation of the hydrophobic chain length show that a minimum hydrophobic domain is required to shield the squaramide units from water when a constant hydrophilic domain is maintained for self-assembly. By contrast, significant increases to the hydrophilic chain length of the bolaamphiphile, while keeping the hydrophobic domain constant, results in a transition from fibrillar to spherical nanoscale objects with an alteration in the aggregation mode of the monomers likely due to steric constraints of the oligo(ethylene glycol) chains. By understanding the self-assembly space achievable for these squaramide-based bolaamphiphiles through examining the interplay between various monomer features, we show their distinct effects on the formation of self-assembled nanoparticles with possibilities to modulate their shape and size in water for future applications in the biomedical area.

Received 26th February 2019,
Accepted 15th April 2019

DOI: 10.1039/c9py00310j

rscl.li/polymers

Introduction

Supramolecular self-assembly is a highly attractive method for the preparation of functional nanostructures due to its modular and expeditious nature. Anisotropic, shape-persistent nanostructures can be achieved through the supramolecular polymerization of designed monomer units by non-covalent interactions such as hydrogen-bonding, ionic, π - π and hydrophobic effects.^{1–10} This approach can be useful in the development of therapeutic nanoparticle libraries for drug delivery, where size and shape among other physicochemical properties of the carrier guides their biodistribution, uptake and clearance *in vivo*.^{11–17} However, the rational design of such nanocarriers still remains non-trivial, especially in aqueous media where strong non-covalent interactions are used to aid monomer self-assembly, but also result in the formation of

kinetically trapped products.^{18–25} Hence, more insight into the effect of various monomer features on supramolecular polymerization is necessary to widen their use in biomedical area.

Bolaamphiphiles are self-assembling modules that consist of two hydrophilic domains with a central hydrophobic core and can access a wide range of well-defined nanostructures in solution, such as micelles, vesicles and high aspect ratio assemblies, such as rods, helices or ribbons.^{26–30} When rigid chains or hydrogen bonds are introduced into their structure, a transition from vesicular aggregates to elongated rod-like micelles or supramolecular polymers is observed.^{26,27} To this end, hydrogen-bonding units, such as amides³¹ or ureas^{30,32} are commonly incorporated into the hydrophobic domain, and recently, our group demonstrated the use of squaramides^{33,34} to elicit such morphological transitions. Thus, to maximize the range of morphologies accessible to this class of monomers, understanding the consequence of various attractive and repulsive interactions and their interplay within a given monomer become critical.

Squaramides^{35–38} are minimalistic ditopic hydrogen bonding units that provide unique opportunities for supramolecular polymer construction^{33,34,39,40} with two N–H hydrogen bond donors opposite two C=O hydrogen bond acceptors on a cyclobutenedione ring. Their high synthetic accessibility starting from commercially available squaric esters permits

^aDepartment of Supramolecular and Biomaterials Chemistry, Leiden Institute of Chemistry, Leiden University, P.O. Box 9502, 2300 RA Leiden, The Netherlands. E-mail: r.e.kieltyka@chem.leidenuniv.nl

^bLaboratory of Physical Chemistry, Laboratory of Macromolecular and Organic Chemistry, and Institute of Complex Molecular Systems, Eindhoven University of Technology, P.O. Box 513, 5600 MB Eindhoven, The Netherlands

†Electronic supplementary information (ESI) available: Synthetic routes and details, cryo-TEM, SAXS, and UV-Vis, IR and fluorescence measurements. See DOI: 10.1039/c9py00310j

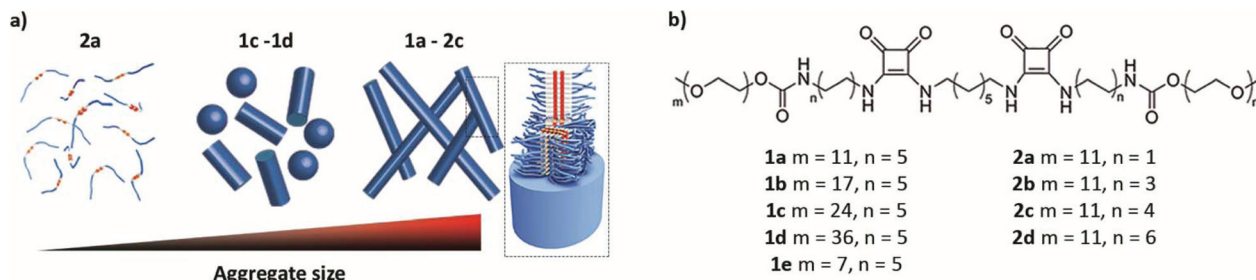


Fig. 1 (a) Schematic representation of morphologies achievable by modulation of the hydrophilic to hydrophobic ratios of the squaramide-based monomers. (b) Chemical structures of the squaramide-based bolaamphiphiles examined in this study.

their facile incorporation into a wide range of polymer structures.^{34,41–43} Previously, our group reported the incorporation of two squaramide synthons into an aliphatic core of a bolaamphiphilic monomer flanked by two undeca(ethylene glycol) chains that form supramolecular polymers on the order of several hundreds of nanometers in water (**1a**, weight fraction of oligo(ethylene glycol) (ω_{OEG}) = 0.60) (Fig. 1).^{33,34} We herein further examine the self-assembly scope of this squaramide-based bolaamphiphile by modulating the size of the linear hydrophilic and hydrophobic domains and probe their effect on the morphology and size of the resultant supramolecular polymer nanoparticles from the molecular to the nanoscale.

Results and discussion

The influence of the hydrophilic chains on the self-assembly of squaramide-based bolaamphiphiles was examined by synthesizing derivatives with 17 (**1b**, ω_{OEG} = 0.70), 24 (**1c**, ω_{OEG} = 0.76), and 36 (**1d**, ω_{OEG} = 0.83) and 7 (**1e**, ω_{OEG} = 0.50) oligo(ethylene glycol) repeat units while maintaining the aliphatic chain length constant ($n = 5$) between this domain and the squaramide units (Fig. 1 and Table 1). Secondly, the contribution of the hydrophobic domain of the bolaamphiphile was studied by modifying the aliphatic spacer between the hydrophilic chain and the squaramide motifs with 2 (**2a**, ω_{OEG} = 0.69), 6 (**2b**, ω_{OEG} = 0.64), 8 (**2c**, ω_{OEG} = 0.62) and 12 (**2d**, ω_{OEG} = 0.58) methylene repeat units, while keeping the remainder of

the hydrophobic and hydrophilic undeca(ethylene glycol) chains lengths constant. An analogous synthetic approach to **1a** was used to prepare the squaramide-based bolaamphiphile library with moderate yields over the various steps (see ESI†). Optically clear solutions ($c = 580 \mu\text{M}$) of the various bolaamphiphiles were obtained when the compounds were dissolved in water, except for **1e** that required sonication. This compound was abandoned for further study and the remaining samples were left to stand 24 hours prior to measurement.

Cryogenic transmission electron microscopy (cryo-TEM) was used as a first approach to probe the effect of modulating the hydrophobic and hydrophilic domains of the bolaamphiphiles on the supramolecular polymer structure (Fig. 2 and ESI, Table 1†). Morphologically distinct self-assembled structures were obtained with systematic modification of the hydrophilic chain length. Samples of **1a** displayed almost exclusively stiff high aspect ratio fibers, while **1b** predominantly displayed elongated fibrillar constructs with a smaller population of shorter, sometimes spherical objects (Fig. 2a and b). The fiber lengths were $234 \pm 108 \text{ nm}$ and $109 \pm 44 \text{ nm}$ for **1a** and **1b**, respectively. However, due to the high dispersity of these samples, fiber-like domains of up to a micron in length could be observed for **1a** and half of this value for **1b**, with comparable diameters of 6–7 nm. Self-assembly of **1c** (Fig. 2c) showed a mixture of spherical aggregates with a diameter of $6 \pm 1 \text{ nm}$ and rod-like aggregates with a length of $57 \pm 24 \text{ nm}$, and is suggestive of kinetic trapping of the bolaamphiphile. For **1d**, only spherical aggregates were found with a diameter of $9 \pm 4 \text{ nm}$ (Fig. 2d). These results suggest that the steric bulk provided by the longer oligo(ethylene glycol) chain lengths can be used to drive the formation of spherical nanoparticles.

Subsequently, the effect of modulating the aliphatic chain length on the self-assembly of **2a–d** was studied (Table 1). No aggregates in solution were observed for **2a** (Fig. 2e). Alternatively, **2b** (Fig. 2f) displayed thin filamentous structures difficult to distinguish from the background, and **2c** (Fig. 2g) exhibited fibrillar objects on the order of $200 \pm 93 \text{ nm}$ and disperse in length with thickness of 5–6 nm. A combination of short rod-like objects and bundles thereof were found for **2d** (Fig. 2h). Thus, bolaamphiphile self-assembly into supramolecular polymers is observed when the aliphatic chains separating the hydrophilic side chains and the squaramide units

Table 1 OEG (ω_{OEG}) weight fraction and morphology as determined from cryo-TEM micrographs of the various squaramide-based supramolecular polymer nanoparticles under study (F – fibrillar, R – rod-like, S – spherical, B – bundles)

Monomer	ω_{OEG}	Morphology
1a	0.60	F
1b	0.70	F
1c	0.76	R/S
1d	0.83	S
2a	0.69	—
2b	0.64	F
2c	0.62	F
2d	0.58	R/B

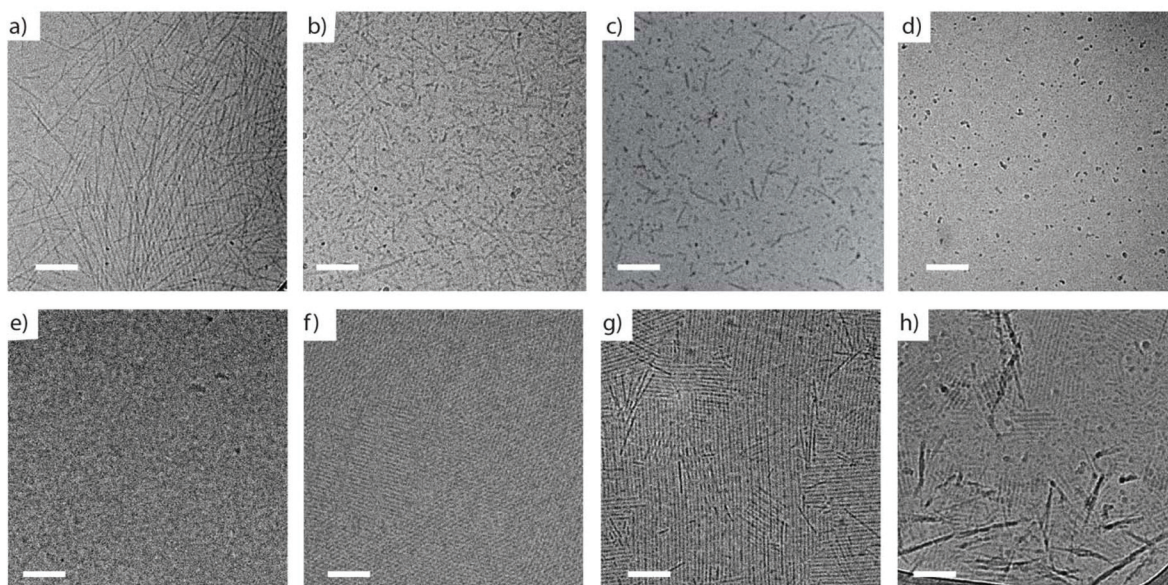


Fig. 2 Cryo-TEM images of squaramide-based bolaamphiphiles in water ($c = 580 \mu\text{M}$). With increasing hydrophilic side chain length and hydrophobic side chain length unchanged: **1a** (a), **1b** (b), **1c** (c), **1d** (d). With increasing hydrophobic side chain length and unchanged hydrophilic side chain length: **2a** (e), **2b** (f), **2c** (g) and **2d** (h). Scale bar: 100 nm.

have at least 8 to 10 methylene repeat units with a fixed undeca(ethylene glycol) chain length.

Small angle X-ray scattering (SAXS) experiments were performed to further characterize the differences in morphology between the various supramolecular polymers prepared from **1a–d**, namely with respect to their size and shape (Fig. 3a and ESI†). For **1a**, we previously reported a SAXS profile characteristic of rod-like structures with a length L outside the accessible q -range. It displays a $I \propto q^{-1}$ power law regime at low q values, followed by a $I \propto q^{-4}$ regime at high q values.³⁴ The experimental data was described with a form factor for rigid, homogenous cylinders yielding a cross-sectional radius of ~ 3.5 nm, which is comparable to the diameter measured by cryo-TEM. We further obtained a cross-sectional mass per unit length (M_L) of $\sim 5.3 \times 10^{20} \pm 0.6 \times 10^{20} \text{ g nm}^{-1}$ from the form factor modeling, which suggests approximately 18–21 squaramide bolaamphiphiles per nm along the fiber. The same model was applied to describe the SAXS profiles of **1b**, providing a r_{cs} of ~ 3.7 nm and a M_L of $\sim 5.9 \times 10^{20} \pm 0.5 \times 10^{20} \text{ g nm}^{-1}$ that translates into a value of roughly 16–20 bolaamphiphiles per nm.

In contrast, **1c** could not be modeled satisfactorily in the same manner. Instead, two form factors (for homogeneous cylinders and spheres) were employed to take the coexistence between fibrils and spherical objects as revealed by cryo-TEM into account. Finally, the sample containing the longest hydrophilic chain, **1d**, gave rise to scattering profiles characteristic of objects with a low aspect ratio. A plateau is found at low q values followed by an $I \propto q^{-4}$ power law regime at high q values. This data set was best modeled with form factors derived for homogeneous and fuzzy spheres,^{44,45} yielding comparable quality of fit and radii of ~ 5.5 nm, providing an esti-

ated overall aggregation number of 31–63 molecules. Hence, small angle X-ray scattering experiments in solution confirm the transition from predominantly fibrillar towards spherical morphologies upon increasing oligo(ethylene glycol) length as seen in the cryo-TEM images.

The self-assembly of the various squaramide-based bolaamphiphiles was further probed at the molecular level by ultraviolet-visible spectroscopy (UV-Vis), fluorescence and IR spectroscopy. Earlier, we reported that self-assemblies of **1a** in water showed UV-Vis maxima at 255 and 329 nm, corresponding to the HOMO–(LUMO+1) and HOMO–LUMO transitions of the squaramide synthon.³⁴ These maxima were largely insensitive to changes in concentration; meanwhile, heating the bolaamphiphiles up to 85 °C or dissolving them in hexafluoroisopropanol (HFIP) (see ESI†), a good solvent for the monomer, resulted in perturbation of these bands and is indicative of their strong aggregation in water. Even with a slightly longer oligo(ethylene glycol) (OEG) chain, **1b** showed a comparable absorption spectrum in water, whereas in spectra of **1c** and **1d** the sharp bands at 255 and 329 nm were of decreased intensity with red and blue-shifts of these maxima, respectively, consistent with a lower degree of polymerization (Fig. 3b). Conversely, decreasing the length of the aliphatic spacer between the squaramide motifs and the hydrophilic oligo(ethylene glycol) chains resulted in even more pronounced differences in the UV-Vis spectra (Fig. 3c). The UV-Vis spectra for **1a–d** and **2a–d** corroborate the aggregate morphologies observed at the nanoscale by cryo-TEM and SAXS.

Temperature-dependent UV-Vis measurements (Fig. 3d) were carried out to gain insight into supramolecular polymerization of **1a**. Heating the fibrillar sample from 25 to 85 °C displayed spectra on par with depolymerization of the supramole-

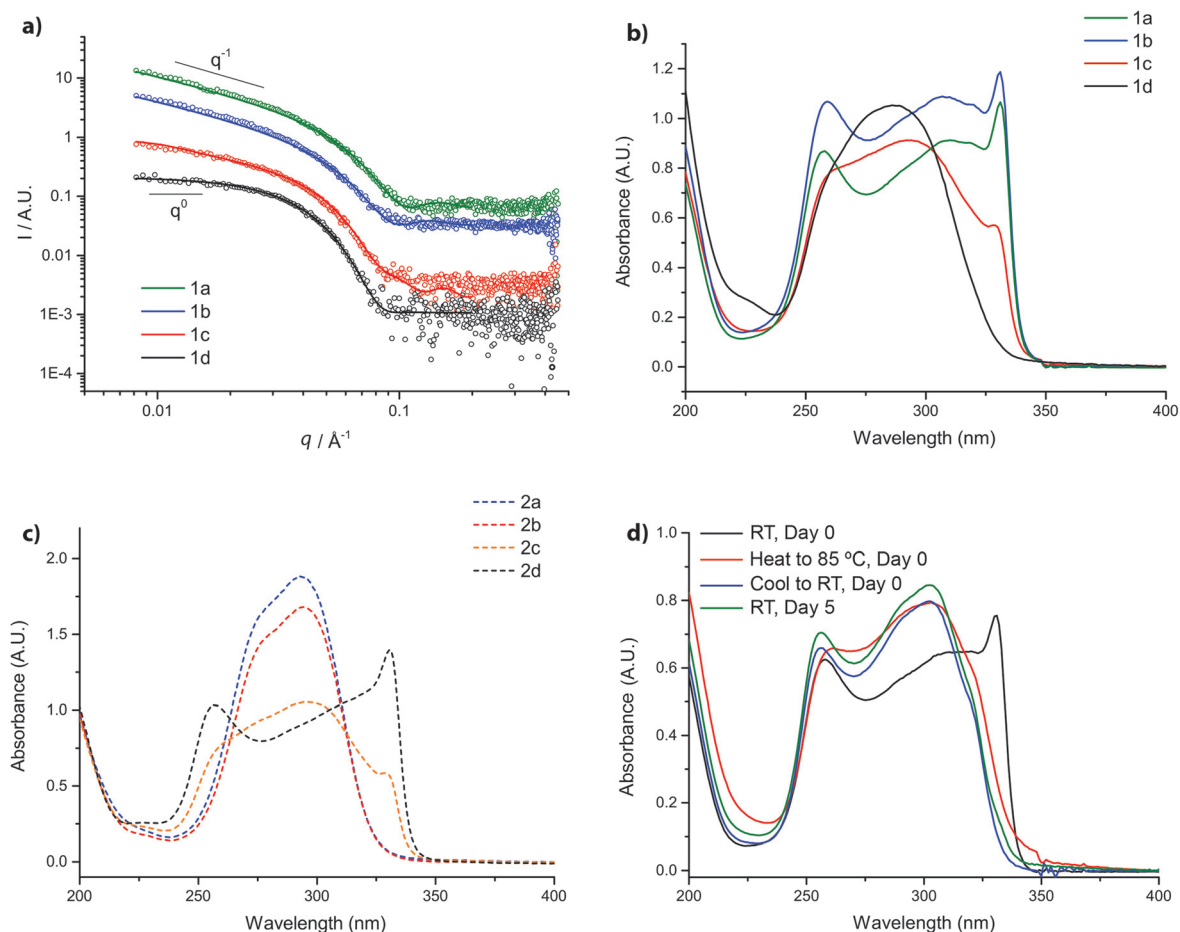


Fig. 3 (a) SAXS profiles for 4 mg mL⁻¹ samples of **1a**, **1b**, **1c** and **1d** in water (circular dots) modelled with a form factor describing a rigid homogeneous cylinder for **1a** and **1b** (green and blue line), two form factors of a describing a homogeneous cylinder and a homogeneous sphere for **1c** (red line) and a form factor of a fuzzy sphere for **1d** (black line). The scattering profiles have been shifted vertically by multiplying by a factor of 2 (red line), 7 (blue line) and 20 (green line). (b, c) UV-Vis absorption traces of (b) **1a–d** and (c) **2a–d** ($c = 30 \mu\text{M}$) in water at room temperature after 24 hours of sample equilibration. (d) UV-Vis spectrum of **1a** at different temperatures: RT, Day 0 (black line), heat to 85 °C, Day 0 (red line), cool to RT, Day 0 (blue line) and RT, Day 5 (green line).

cular polymers. The absorbance at 329 nm, a maximum consistent with the aggregated state, as a function of increasing temperature showed an abrupt decrease in intensity around 60 °C. Upon cooling, this peak showed strong hysteresis and did not return after five days, thus being suggestive of a kinetic process. UV-Vis spectra of **2a** and **2b** bearing 2 and 6 methylenes over several concentrations, respectively, lacked features of squaramide self-assembly in water as observed for the fibrillar aggregates, consistent with cryo-TEM imaging (see ESI†). When the length of the aliphatic spacer was further increased to 8 methylene units, as in **2c**, the onset of a spectral profile similar to that of **1a** was observed. In the case of **2d**, the spectral profile resembled that of **1a** with peaks at 329 and 255 nm, congruent with earlier findings of squaramide self-assembly. Thus, self-assembly of squaramide-based bolaamphiphiles is readily probed by UV-Vis spectroscopy, revealing distinct regimes of polymerization consistent with their molecular structure.

Aggregation of the squaramide-based bolaamphiphiles was further supported by fluorescence measurements using the

Nile red dye (NR, see ESI†). NR is a hydrophobic dye that undergoes a blue shift in its emission maximum at 650 nm and an increase in fluorescence intensity when encapsulated in a hydrophobic environment. This shift thus provides a view into the contribution of the hydrophobic effect to the self-assembly process.⁴⁶ A blue-shift of the emission wavelength and 4 to 5-fold increase in the peak intensity of NR were recorded for **1a–d** when compared against the dye in water as a control (Fig. 4a). The same shift was observed for **1a** and **1b**, $\Delta\lambda_{\text{max}} = -35$ nm, while **1c** presented a $\Delta\lambda_{\text{max}} = -26$ nm and **1d** a $\Delta\lambda_{\text{max}} = -21$ nm, consistent with a decrease in the hydrophobic character of the bolaamphiphile with increasing oligo (ethylene glycol) length. Conversely, for **2a–d** a gradual increase in the fluorescence intensity is measured with the increased length of the aliphatic spacer, as expected (Fig. 4b). An emission peak was recorded for **2a** on par with that of the NR dye in water, whereas shifts of $\Delta\lambda_{\text{max}}$ of -10 , -18 and -38 nm were measured for **2b**, **2c** and **2d**, respectively, with a 6-fold increase in the intensity for the latter. The fluorescence

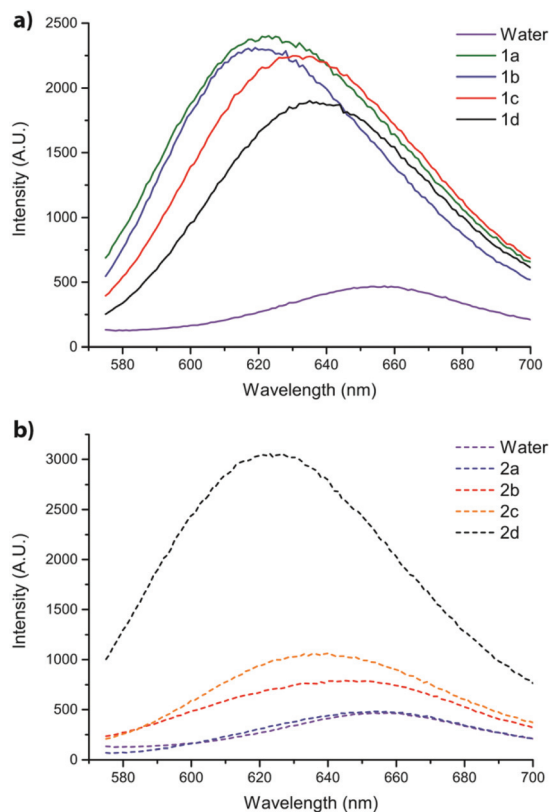


Fig. 4 Fluorescence spectra of NR (ex. = 550 nm) with **1a–e** (a) and **2a–d** (b) in aqueous solution ($c = 30 \mu\text{M}$).

results support the aggregation of the squaramide-based bolaamphiphiles in UV-Vis measurements and their respective trends when altering their hydrophobic and hydrophilic domains.

Fourier transform infrared (FTIR) spectroscopy was used to investigate the hydrogen bonding in the various squaramide-based supramolecular polymer nanoparticles. For compound **1a**, we earlier reported the N–H stretch at 3162 cm^{-1} and C=O stretches at 1687 , 1676 and 1642 cm^{-1} for the squaramide and carbamate moieties of the squaramide-based bolaamphiphile when self-assembled in water, while a small broad peak at 1796 cm^{-1} was assigned to the ring breathing of the squaramide moiety.³⁴ The features of the IR spectrum were largely unchanged with decreasing concentration, except for its intensity. When the temperature was increased from 25 to $65 \text{ }^\circ\text{C}$ (Fig. 5) in water, a shift to higher wavenumbers of the N–H peak of **1a** of 3 cm^{-1} with a decrease in its intensity with concomitant changes in the carbonyl region were observed, indicative of hydrogen-bonding between bolaamphiphiles. Through increasing the oligo(ethylene glycol) chain length (**1b** to **1d**), the N–H stretch peak becomes bimodal and decreases in intensity towards the baseline. In the carbonyl region, similar patterns of bands are observed for **1a** and **1b**, and **1c** and **1d** (Fig. 6a). The spectral differences between these two sets of bolaamphiphiles in the C=O and N–H regions are thus suggestive of a distinct mode of aggregation between both pairs. Subsequently, we measured samples **1b–d** in HFIP- d_2

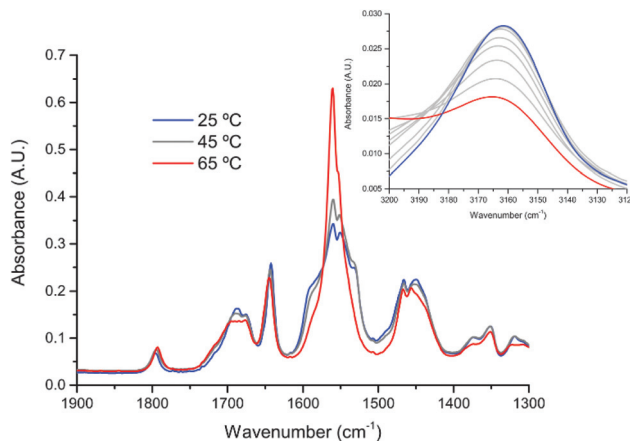


Fig. 5 FTIR spectrum of **1a** in D_2O with increasing temperature from $25 \text{ }^\circ\text{C}$ (blue line) to $65 \text{ }^\circ\text{C}$ (red line). Inset: NH region ($3200\text{--}3120 \text{ cm}^{-1}$).

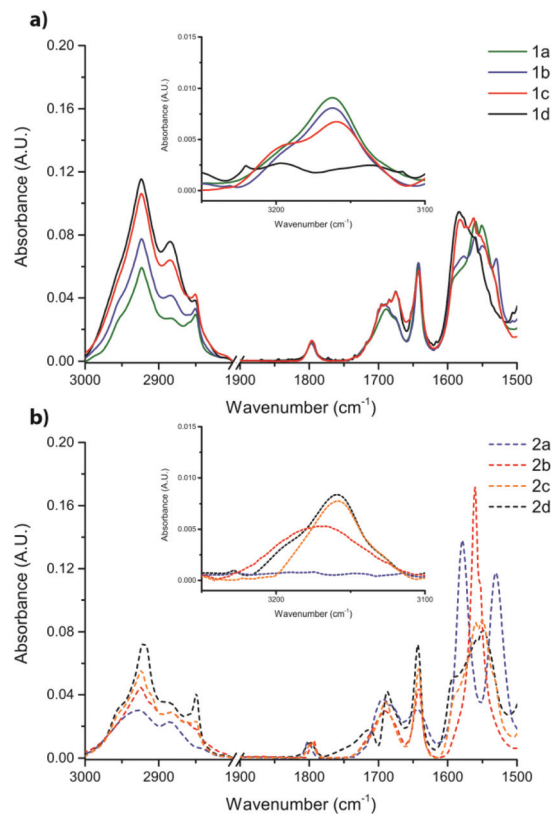


Fig. 6 FTIR spectra of **1a–d** (a) and **2a–d** (b) in D_2O ($c = 5.8 \text{ mM}$). N–H (inset), amide I and amide II regions are plotted.

(see ESI[†]). As expected, loss of the N–H stretch was observed for **1b–d** due its likely superposition with the O–H stretch. The ring breathing peak and the C=O stretches of the squaramide synthon in the amide I region were shifted to higher wavenumbers by $10\text{--}15 \text{ cm}^{-1}$ and decreased in intensity with the addition of HFIP- d_2 , consistent with disassembly of the supramolecular polymer. The IR results suggest a distinct aggregation mode between **1a** and **1b**, and **1c** and **1d** due to the

increased length of the oligo(ethylene glycol) chains that impose sterically on the formation of supramolecular polymers.

IR studies were also carried out on **2a–d** where the eventual formation of fibrillar aggregates in water was observed. The gradual appearance of a vibration at 3162 cm^{-1} was observed when comparing the N–H stretches (inset Fig. 6b) of **2a** and **2d**. This result is consistent with the increased hydrophobic shielding of the squaramide units from their aqueous surroundings with lengthening of the aliphatic spacer. In the amide II region, **2a** showed two sharp peaks at 1578 cm^{-1} and 1530 cm^{-1} , similar to those found for **2a** when dissolved in HFIP- d_2 and absent in **2b–d**. Moreover, a gradual increase in intensity was observed for the carbonyl stretch of the squaramide at 1643 cm^{-1} and the ring breathing peak moved to lower wavenumbers (from 1801 cm^{-1} for **2a** to 1797 cm^{-1} for **2d**), consistent with their polymerization upon increasing aliphatic chain length. Thus, a lesser degree of aggregation is observed when increasing the length of the hydrophilic oligo(ethylene glycol) chains from 11 to 36 repeat units, while 8 methylene repeat units in the aliphatic spacer within the bolaamphiphile are optimal to facilitate the interaction between the squaramides by hydrogen bonding.

Conclusion

Systematic chemical modifications of a squaramide-based bolaamphiphile at its linear hydrophilic side chains (**1a–e**) and hydrophobic core (**2a–d**) revealed distinct effects on their supramolecular polymerization. A minimum hydrophobic chain length of 8 carbons between the squaramide and a fixed undeca(ethylene glycol) chain length was required to ensure the formation of fibrillar aggregates. On the other hand, increasing the hydrophilic oligomer chain length (up to $m = 36$), while maintaining the same aliphatic chain length constant of 10 carbons, was found to guide a morphological transition from fibrillar to spherical aggregates likely due to increased steric demand of the linear hydrophilic oligomer chains. Consequently, a distinct packing mode of monomer within the aggregate structure was observed spectroscopically, but the precise nature of their self-assembly within the spherical aggregates is unknown; whether they are in a bent or straight conformation.²⁷ Importantly, the ability to achieve a range of nanoparticle morphologies that transition from sphere to fibers by tuning the same building blocks renders the formed scaffolds highly attractive for fundamental and applied research in the field of nanomedicine.

Experimental

Materials and methods

All solvents and reagents were obtained from commercial suppliers and were used without further purification. Oligo(ethylene glycol) methyl ether(s) were obtained from Polypure and

Broadpharm. Deuterated dimethylsulfoxide and chloroform were purchased from Euriso-top. Palladium on matrix activated carbon, triethylsilane, deuterium oxide, hexafluoroisopropanol and all other commercial grade reagents and chemicals were purchased from Sigma Aldrich and used as received. Milli-Q water was used for all the studies. Full synthetic routes and details for compounds **1a–d** and **2a–d** can be found in the ESI.†

Cryogenic transmission electron microscopy

Cryogenic transmission electron microscopy (cryo-TEM) samples were applied to freshly glow-discharged Lacey Carbon Film (300 mesh Cu grids) and plunge-frozen in liquid ethane using a Leica EM GP. Images were recorded with a Tecnai F20 FEG (FEI company, The Netherlands), equipped with a field emission gun at 200 keV using a GatanUltraScan camera (Gatan company, Germany) with a defocus between -3 and $-9\text{ }\mu\text{m}$. The samples were prepared by applying three microliters of sample solution ($580\text{ }\mu\text{M}$) to a freshly glow-discharged Lacey Carbon Film (300 mesh Cu grids). The excess of liquid was blotted away for 1 second (95% humidity, RT, Whatman no. 4 filter paper) and plunge-frozen in liquid ethane at $-183\text{ }^\circ\text{C}$ using a Leica EM GP. The obtained cryo-TEM images were analyzed using the “Fiji” image processing software. Samples **1a**, **1b**, **1c**, **1d** and **2c** were analyzed. The length and width of 50 aggregates were measured per sample. Values are expressed as the average \pm their standard deviation (see histograms in Fig. S1–S5†).

Small angle X-ray scattering (SAXS)

Small angle X-ray scattering (SAXS) measurements were carried on a SAXSLAB GANESHA 300 XL SAXS system equipped with a GeniX 3D Cu Ultra Low Divergence micro focus sealed tube source producing X-rays with a wavelength $\lambda = 1.54\text{ }\text{Å}$ at a flux of 1×10^8 ph per s and a Pilatus 300 K silicon pixel detector with 487×619 pixels of $172\text{ }\mu\text{m} \times 172\text{ }\mu\text{m}$ in size placed at two sample-to-detector distances of 713 and 1513 mm respectively to access a q -range of $0.006 \leq q \leq 0.44\text{ }\text{Å}^{-1}$ with $q = 4\pi/\lambda(\sin \theta/2)$. Silver behenate was used for calibration of the beam center and the q range. Samples were contained at room temperature in 2 mm quartz capillaries (Hilgenberg GmbH, Germany). The two-dimensional SAXS patterns were brought to an absolute intensity scale using the calibrated detector response function, known sample-to-detector distance, measured incident and transmitted beam intensities, and azimuthally averaged to obtain one dimensional SAXS profiles. The scattering curves of the self-assembled structures were obtained by subtraction of the scattering contribution of the solvent and quartz capillary. The small angle X-ray scattering profiles were analyzed using the software package SasView (<http://www.sasview.org/>). Small angle X-ray scattering (SAXS) experiments were performed on aqueous solutions of the monomers **1a**, **1b**, **1c** and **1d** to study their progressive transition from fiber-like to spherical aggregates upon increasing the length of the hydrophilic segment. All SAXS measurements were carried out in MQ water at room temperature.

UV-Vis spectroscopy

Absorption spectra were obtained on a Cary 300 UV-Vis spectrophotometer. All measurements were carried out using a quartz cuvette with a 1 cm path length. UV-Vis samples were prepared from stock solutions of the various squaramide-based bolaamphiphiles **1a-d** and **2a-d** (5.8 mM) equilibrated overnight prior to their dilution at the measuring concentration (30 μM).

Fluorescence measurements

Fluorescence spectra were acquired on a Tecan Plate Reader Infinite M1000 using 96 well plates (PP Microplate, solid F-bottom (flat), chimney well). Solutions of the various squaramide-based bolaamphiphiles from compounds **1a-d** and **2a-d** (5.8 mM) were prepared in D_2O and HFIP- d_2 and left to equilibrate overnight before measurement. A stock solution of Nile Red (15 μM) in CH_3OH was spotted (7 μL) in the wells of a 96-well plate (PP Microplate, solid F-bottom (flat), chimney well) and was placed under vacuum for at least four hours to remove the solvent. The various squaramide-based bolaamphiphiles (stock solution: 30 μM) were added (100 μL) to the wells pre-spotted with Nile Red. The solutions were shaken vigorously in the Tecan plate reader (300 seconds, 654 rpm, linear mode) and then allowed to equilibrate overnight at room temperature. Fluorescence measurements were collected at excitation wavelength of 550 nm and an emission wavelength from 570 to 700 nm.

IR spectroscopy

Transmission FTIR spectra were measured using a Bio-Rad Excalibur spectrometer equipped with a nitrogen-cooled MCT detector. A liquid transmission cell with CaF_2 windows and a fixed nominal path length of 50 mm was used. Sample spectra were recorded in deuterated solvents at room temperature, with a resolution of 1 cm^{-1} . For each spectrum 128 scans were averaged. The final absorbance spectrum was expressed in terms of absorbance and corrected by manual subtraction of a water vapor spectrum. Baseline was subtracted and brought to a zero value by using Origin 9.1 software.

Conflicts of interest

There are no conflicts to declare.

Acknowledgements

We thank T. Sharp, R. I. Koning and B. Koster (cryoTEM). R. E. K. (NWO-ECHO-STIP Grant 717.014.005, NWO-VENI Grant 722.012.011) would like to thank the Netherlands Organization for Scientific Research (NWO) for financial support.

Notes and references

- 1 T. Aida, E. W. Meijer and S. I. Stupp, *Science*, 2012, **335**, 813.
- 2 E. Krieg, M. M. C. Bastings, P. Besenius and B. Rybtchinski, *Chem. Rev.*, 2016, **16**, 2414.
- 3 C. Schmuck, *Nat. Nanotechnol.*, 2011, **6**, 136.
- 4 H.-W. Schmidt, *Angew. Chem., Int. Ed.*, 2012, **51**, 10933.
- 5 M. R. Chierotti and R. Gobetto, *Supramol. Chem.: Mol. Nanomater.*, 2012, 4014.
- 6 L. E. Buerkle and S. J. Rowan, *Chem. Soc. Rev.*, 2012, **41**, 6089.
- 7 J.-M. Lehn, *Angew. Chem., Int. Ed. Engl.*, 1990, **29**, 1304.
- 8 J. Boekhoven and S. I. Stupp, *Adv. Mater.*, 2014, **26**, 1642.
- 9 T. F. A. de Greef and E. W. Meijer, *Nature*, 2008, **453**, 171.
- 10 T. F. A. de Greef, M. M. J. Smulders, M. Wolffs, A. P. H. J. Schenning, R. P. Sijbesma and E. W. Meijer, *Chem. Rev.*, 2009, **109**, 5687.
- 11 A. S. Hoffman, *J. Controlled Release*, 2008, **132**, 153.
- 12 S. Venkataraman, J. L. Hedrick, Z. Y. Ong, C. Yang, P. L. R. Ee, P. T. Hammond and Y. Y. Yang, *Adv. Drug Delivery Rev.*, 2011, **63**, 1228.
- 13 M. J. Webber and R. Langer, *Chem. Soc. Rev.*, 2017, **46**, 6600.
- 14 E. A. Simone, T. D. Dziubla and V. R. Muzykantov, *Expert Opin. Drug Delivery*, 2008, **5**, 1283.
- 15 M. J. Webber, E. A. Appel, E. W. Meijer and R. Langer, *Nat. Mater.*, 2015, **15**, 13–26.
- 16 M. F. Bachmann and G. T. Jennings, *Nat. Rev. Immunol.*, 2010, **10**, 787.
- 17 R. A. Petros and J. M. DeSimone, *Nat. Rev. Drug Discovery*, 2010, **9**, 615.
- 18 Y. Yan, J. Huang and B. Z. Tang, *Chem. Commun.*, 2016, **52**, 11870.
- 19 A. G. Denkova, E. Mendes and M. O. Coppens, *Soft Matter*, 2010, **6**, 2351.
- 20 R. Appel, J. Fuchs, S. M. Tyrell, P. A. Korevaar, M. C. A. Stuart, M. Schonhoff and P. Besenius, *Chem. – Eur. J.*, 2015, **21**, 19257.
- 21 J. Baram, H. Weissman and B. J. Rybtchinski, *J. Phys. Chem. B*, 2014, **118**, 12068.
- 22 T. Miti, M. Mulaj, J. D. Schmit and M. Muschol, *Biomacromolecules*, 2015, **16**, 326.
- 23 C. M. A. Leenders, M. B. Baker, I. A. B. Pijpers, R. P. M. Lafleur, L. Albertazzi, A. R. A. Palmans and E. W. Meijer, *Soft Matter*, 2016, **12**, 2887.
- 24 P. Rajdev, S. Chakraborty, M. Schmutz, P. Mesini and S. Ghosh, *Langmuir*, 2017, **33**, 4789.
- 25 P. Dey, P. Rajdev, P. Pramanik and S. Ghosh, *Macromolecules*, 2018, **51**, 5182.
- 26 N. Nuraje, H. Bai and K. Su, *Prog. Polym. Sci.*, 2013, **38**, 302.
- 27 J. H. Fuhrhop and T. Wang, *Chem. Rev.*, 2004, **104**, 2901.
- 28 A. Pal, S. Karthikeyan and R. Sijbesma, *J. Am. Chem. Soc.*, 2010, **132**, 7842.
- 29 T. Rudolph, N. Kumar Allampally, G. Fernández and F. H. Schacher, *Chem. – Eur. J.*, 2014, **20**, 13871.
- 30 E. Obert, M. Bellot, L. Bouteiller, F. Andrioletti, C. Lehen-Ferrenbach and C. F. Boué, *J. Am. Chem. Soc.*, 2007, **129**, 15601.

- 31 T. Shimizu, R. Iwaura, M. Masuda, T. Hanada and K. Yase, *J. Am. Chem. Soc.*, 2001, **123**, 5947.
- 32 M. Fernandez-Castano Romera, R. P. M. Lafleur, C. Guibert, I. K. Voets, C. Storm and R. P. Sijbesma, *Angew. Chem., Int. Ed.*, 2017, **56**, 8771.
- 33 W. E. M. Noteborn, V. Saez Talens and R. E. Kieltyka, *ChemBioChem*, 2017, **18**, 1995.
- 34 V. Saez Talens, P. Englebienne, T. T. Trinh, W. E. M. Noteborn, I. K. Voets and R. E. Kieltyka, *Angew. Chem., Int. Ed.*, 2015, **54**, 10505.
- 35 R. Ian Storer, C. Aciro and L. H. Jones, *Chem. Soc. Rev.*, 2011, **40**, 2330.
- 36 J. Alemán, A. Parra, H. Jiang and K. A. Jørgensen, *Chem. – Eur. J.*, 2011, **17**, 6890.
- 37 D. Quiñonero, A. Frontera, P. Ballester and P. M. Deyà, *Tetrahedron Lett.*, 2000, **41**, 2001.
- 38 D. Quiñonero, R. Prohens, C. Garau, A. Frontera, P. Ballester, A. Costa and P. M. Deyà, *Chem. Phys. Lett.*, 2002, **351**, 115.
- 39 C. López, M. Ximenis, F. Orvay, C. Rotger and A. Costa, *Chem. – Eur. J.*, 2017, **23**, 7590.
- 40 C. Tong, T. Liu, V. Saez Talens, W. E. M. Noteborn, T. H. Sharp, M. M. R. M. Hendrix, I. K. Voets, C. L. Mummery, V. V. Orlova and R. E. Kieltyka, *Biomacromolecules*, 2018, **19**, 1091.
- 41 F. R. Wurm and H. A. Klok, *Chem. Soc. Rev.*, 2013, **42**, 8179.
- 42 L. Martínez, G. Martorell, Á. Sampedro, P. Ballester, A. Costa and C. Rotger, *Org. Lett.*, 2015, **17**, 2980.
- 43 J. Schiller, J. V. Alegre-Requena, E. Marqués-López, R. P. Herrera, J. Casanovas, C. Alemán and D. Díaz Díaz, *Soft Matter*, 2016, **12**, 4361.
- 44 S. Rathgeber, M. Monkenbusch, M. Kreitschmann, V. Urban and A. Brulet, *J. Chem. Phys.*, 2002, **117**, 4047.
- 45 M. Stieger, J. S. Pedersen, P. Lindner and W. Richtering, *Langmuir*, 2004, **20**, 7283.
- 46 M. C. A. Stuart, J. C. Van De Pas and J. B. F. N. Engberts, *J. Phys. Org. Chem.*, 2005, **18**, 929.